EPS Metop-B Product Validation Report: GRAS

Doc.No. : EUM/OPS-EPS/DOC/12/0663
Issue : v3
Date : 21 January 2013

EUMETSAT
EUMETSAT Allee 1, D-64295 Darmstadt, Germany
Tel: +49 6151 807-7
Fax: +49 6151 807 555
http://www.eumetsat.int

This page has been left blank

Document Change Record

Issue / Revision	*Date*	*DCN. No*	*Changed Pages / Paragraphs*
v1	27 Sep 2012		First issue for trial dissemination
v2	25 Oct 2012		Issue for pre-operational validation status
v3	21 Jan 2013		Issue for Publication

Table of Contents

1 INTRODUCTION

1.1 Purpose and Scope

This Product Validation Report provides the results of the validation testing of the following product(s) in the context of the EUMETSAT Polar System (EPS) Metop-B satellite commissioning:

- GRAS Level 1b

The Metop-B satellite has been launched from Baikonur on September 17th, 2012. The satellite commissioning including Cal/Val testing aims at verifying the capability of the satellite and ground segment to provide operational services with the required levels of availability, timeliness and quality. In particular, the main objective of Cal Val is to ensure that the quality of the products satisfies the operational requirements.

This report is submitted to the Product Validation Review Board in order to decide on the validation status of the GRAS Level 1b products. It is intended for users of GRAS products, the members of the Science and Products Validation Team (SPVT), and for the Metop-B commissioning management.

1.2 Applicable and Reference Documents

1.2.1 Applicable Documents

AD-1	EPS Program GRAS Metop-B Calibration and Validation Plan, EUM/MET/TEN/10/0159
AD-2	EPS Programme Calibration and Validation Overall Plan, EUM.EPS.SYS.PLN.02.004

1.2.2 Reference Documents

RD-1	EPS Metop-B Product Validation Report: GRAS v1 (28.09.2012), EUM/OPS-EPS/DOC/12/0663 v1
RD-2	Calibration-Validation Activities for Metop-B, A. Hausschild, DLR/ESOC, 4.10.2012 (HB # 440567)
RD-3	Metop-B GRAS: Comparison of EUMETSAT Product with Météo-France Model, N. Saint-Ramond, Météo-France, 19.10.2012 (HB # 440568)

1.3 Description of Validation Environment

The baseline for product validation is the operational processing as run in the EPS Core Ground Segment (CGS), in particular

- EPS GS1 running GRAS PPF v2.19 (Metop-A and Metop-B)

Results of the Precise Orbit Determination (POD) run as part of the operational GRAS processing as well as the quality of operational products generated in the EPS CGS are regularly monitored in the GRAS Monitoring Facility run in EUMETSAT's Technical Computing Environment (TCE), which is an integrated part of the GRAS prototype

- YAROS v0.8.4-dev (rev. 2560 / 14-08-2012),

exploiting

- NAPEOS v3.5E (rev. 84 / 23-03-2012)
- NAPEOS Scenarios v3.5E (rev. 72 / 10-08-2012)

for POD monitoring.

Due to limitations of the operational processing chain, most aspects of low level data quality cannot be analyzed based on PPF products; there is also no attempt to process raw sampling data in the current operational processing. Neither known shortcomings in raw GRAS data (like data gaps in rising occultations) nor standard quality control data like Signal-to-Noise ratios (SNR) can be analysed based on PPF output. Therefore, results from the GRAS prototype processing are also contained in this report in as much as they provide additional insight into GRAS-B data quality. The prototype processing is based on

- YAROS v0.8.4-dev (rev. 2535 / 17-07-2012)

using

- NAPEOS v3.5E (rev. 84 / 23-03-2012)
- NAPEOS Scenarios v3.5E (rev. 72 / 10-08-2012)

for all POD purposes.

The versions of all software tools are identical to those used in the PVRB Report RD-1 supporting the approval of a trial dissemination to selected validation partners[1].

[1] The revision of the NAPEOS Scenarios was erroneously given as "rev 62 (13-03-2012) in the PVRB Report for the trial dissemination due to a mistake of the author. Manual inspection of the file system showed that the Napeos configuration database has not changed since the beginning of the Metop-B SIOV.

2 INTERNAL EUMETSAT VALIDATION

2.1 Operational Processing

2.1.1 Data Availability

The first GRAS-B science data became available from sensing times 08:21:02 UTC on 24. September 2012 onwards, shortly after the GRAS instrument had been put into navigation and, subsequently, occultation measurement mode at 08:20:47 UTC and 08:21:47 UTC, respectively. Since then, the GRAS instrument has continuously provided data.

The data was initially processed on GS2 only; data processing on GS1 was activated on the following day (25.09.2012) starting with measurements taken at 12:39 UTC. In the first version of this report, the analysis of operational GRAS products was therefore primarily based on GS2 data, and provided additional evidence that the data quality is consistent on both GS2 and GS1.

Processing on GS1 has been uninterrupted since the availability of the first GRAS data. This version of the report is therefore exclusively based on data processed on GS1.

2.1.2 Processing

A manual inspection of log files and the node-local monitoring database of the GRAS PPF has been carried out on irregular occasions and confirmed showed that the GRAS PPF successfully processes GRAS-B data since it became available. In particular,

- measurement reconstruction from level0 data files succeeded;
- precise orbit determination achieved convergence after the beginning of the processing as well as after the various manoeuvres carried out (a sequence of drift stop manoeuvres on 27. and 28.09.2012 as well as a collision avoidance manoeuvre on 23.10.2012);
- both level 1a and 1b products (if occultation data available within any PDU processing period) were generated successfully;
- level 1b data products were (as expected) flagged as containing “degraded bending angle data” for the first 4 hours after the initial POD step and individual manoeuvres;
- level 1b data products were successfully converted into bufr products by FIST.

We note that a small number of level 1b products from both Metop-A and –B triggered a well-known bug in FIST (EUM/EPS/AR/13718); the software is awaiting an update fixing this problem after the end of the freeze of the EPS ground segment. As both Metop-A and –B products are affected in similar numbers, and as the issue has been known and accepted for several months, it is not considered to affect the operational readiness of GRAS-B data.

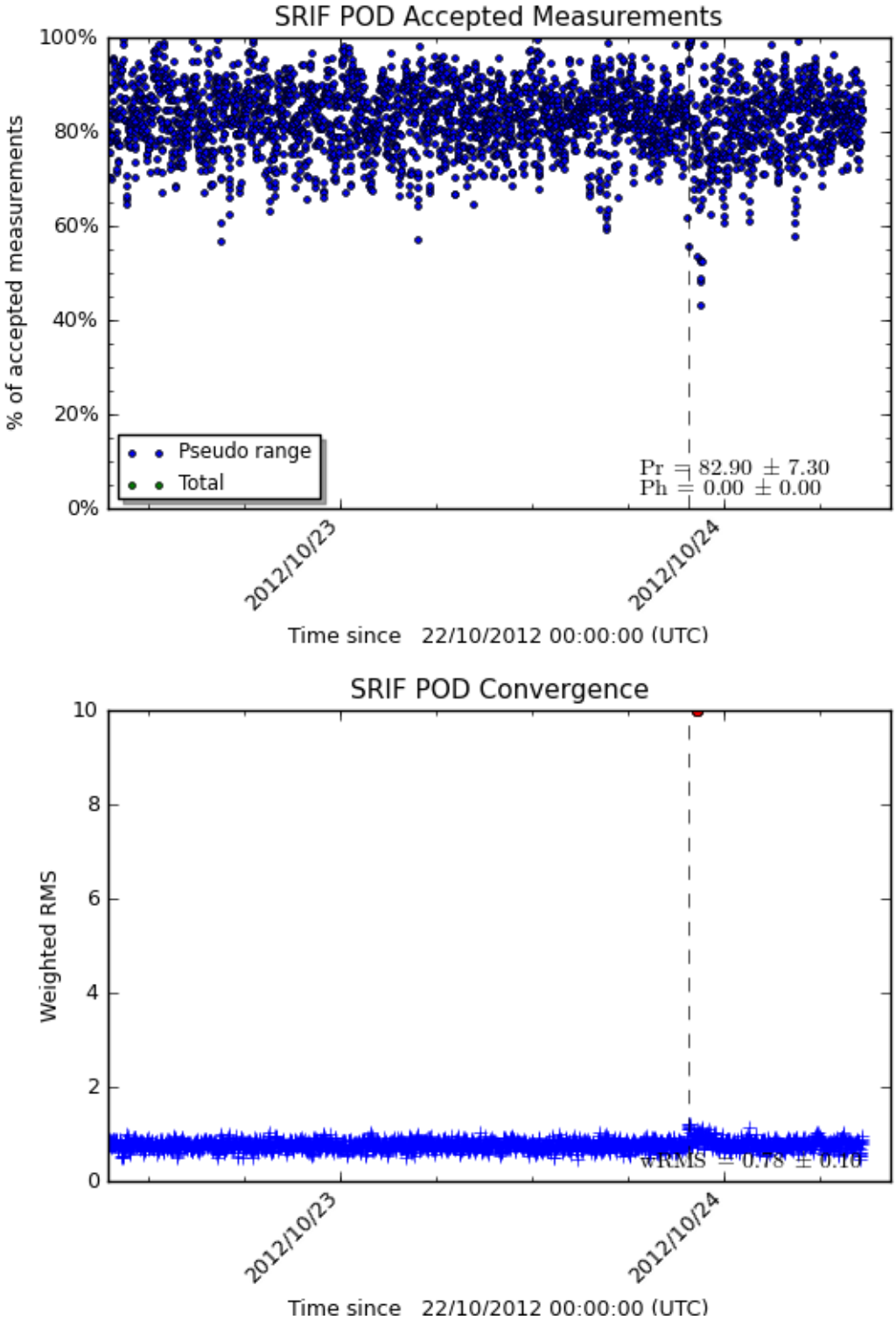

Figure 1: Percentage of accepted (pseudo range) measurements (top) and weighted RMS of the observation residuals (bottom) for the first stage (position run) SRIF POD during 48 hours of Metop-B data (from 22nd to 24th Oct 2012). The dashed vertical line denotes a POD reset triggered due to the METOP-B collision avoidance manoeuvre carried out at 21:41 UTC on 23rd Oct 2012.

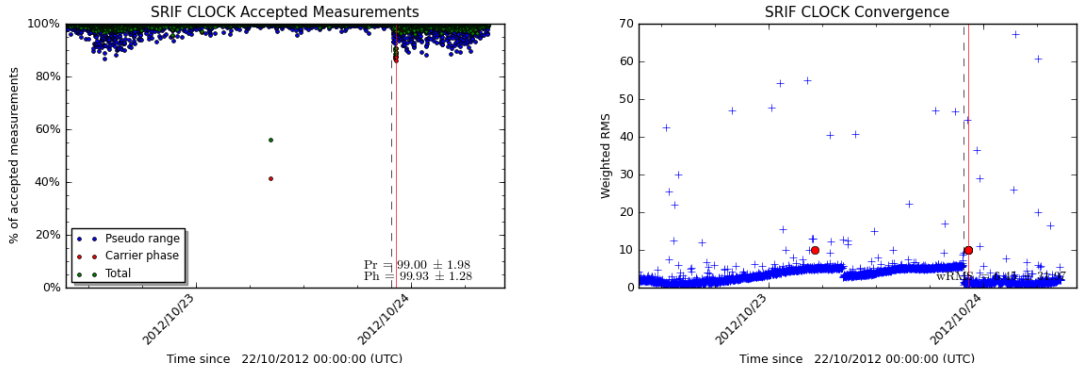

Figure 2: As Figure 1, but for the second stage (clock run) of the SRIF POD. Percentage of accepted observations is shown on the left, weighted RMS on the right. The vertical lines indicate POD reset associated with the collision avoidance manoeuvre on 23rd October (dashed) and a clock processing anomaly (red) shortly afterwards; see text for details.

2.1.3 POD Performance

The Precise Orbit Determination in the operational GRAS PPF is based on a sequential Square-Root Information Filter (SRIF) exploiting a two-step process: In a first run, the previously estimated position of the Metop satellite is updated using pseudo range observations only, while clock bias and drift estimates are updated in a second run by exploiting both pseudo range and carrier phase measurements. As part of the node-local monitoring database of the GRAS PPF, statistics from both POD steps is collected for monitoring purposes.

Figure 1 shows the percentage of observations accepted by the position run as well as the weighted RMS of the pseudo range observations for a recent 48 hour period of Metop-B data (from 22nd to 24th October 2012). Both the number of 80%+ accepted measurements as well as a weighted RMS below are consistent with the expectations for the positioning run, and moreover similar to results typically obtained in the operational processing of Metop-A data. The figure also shows the behaviour of the operational POD during the collision avoidance manoeuvre which had to be carried out at 21:41 UTC on 23rd October; a manual reset (indicated by the dashed vertical line) of the operational POD was triggered one minute after the manoeuvre, and led to the quick re-convergence of the Metop-B precise orbit. Similar patterns – including those during manoeuvres – are observed and well known from the processing of Metop-A data.

Equivalent diagnostics from the second (clock) run shown in Figure 2 also show the typical patterns well known from Metop-A processing: with increasing time, more and more observations are getting accepted in the clock estimation, yielding slowly increasing measurement residuals. This behaviour is caused by noise from observations being mapped into clock bias noise rather than being rejected. This happens because clock bias estimates in a precise orbit determination are significantly less strictly constrained physically compared to, e.g., satellite positions and velocities. Weighted RMS values in the order of several 10 are

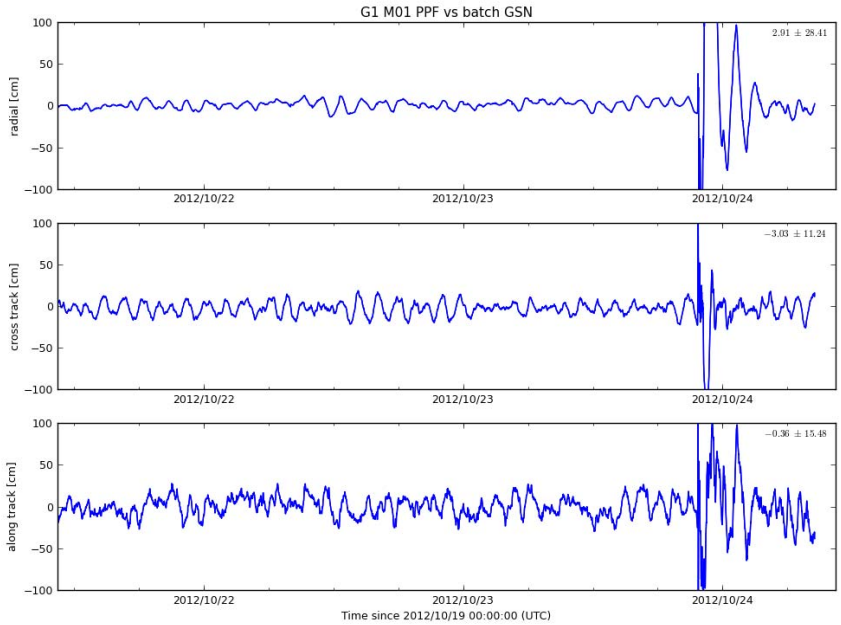

Figure 3: Time series of position differences (from top to bottom: radial, along-track and cross-track deviation, in cm) between operational and offline/monitoring POD for Metop-B between 21st and 24th October 2012. Note the signature of the re-convergence of the operational SRIF solution after the manoeuvre on 23rd October.

also frequently observed in the Metop-A processing, as is the anti-correlation between weighted RMS and percentage of observations accepted in the estimation.

An interesting feature can be observed shortly after the manoeuvre on 23rd October, where the clock run failed with an error (denoted by the red vertical line). Although a detailed investigation is still pending, the pattern reminds of an anomaly (EUM/EPS/AR/11133) where the phase locked loop of the ultra-stable GRAS clock oscillator experiences a slip, resulting in a finite clock jump which cannot be handled by the current operational GRAS PPF. This event occurs rarely, and its re-occurrence for GRAS-B had to be expected; it is therefore not considered critical for the operational readiness of GRAS-B level 1 products.

In summary therefore, the monitoring information collected from both the position and clock estimate runs is consistent with the behaviour observed in the operational GRAS-A processing. This confirms that the POD for GRAS-B data has been performing as expected, and should have produced nominal orbit data.

Most critical for the performance of radio occultation products are the deviations of position in the radial direction and – strongly correlated with the latter – the along-track velocity errors of the POD solution. Figure 3 and Figure 4 show time series of the differences in position and velocity between the precise orbit solution as obtained in GS1 and a batch-based precise orbit solution as obtained in the TCE Monitoring Environment for the GRAS processing. In contrast to the operational POD, the monitoring POD is based on a 6 or 24

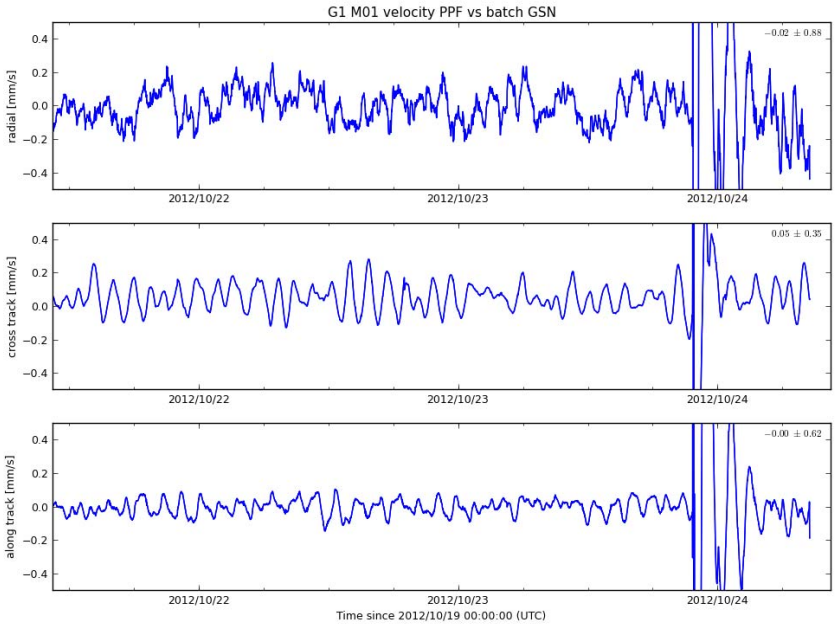

Figure 4: As Figure 3, but for velocity (in mm/s).

hour batch estimation process which is known to be significantly more precise and stable than the sequential POD solution calculated in the operational ground segments.

We note that the re-convergence of the SRIF solution after the collision avoidance manoeuvre carried out at 21:41 UTC on 23rd October is nicely demonstrated in this example. As observed for Metop-A, this converging period typically lasts for about 4 hours, after which the deviations between the orbit solutions become stable in amplitude, exhibiting per-orbit fluctuations. The same qualitative pattern can also be seen in the velocity deviations between the two solutions.

Over the period covered by the statistics shown in Figure 3, the individual components exhibit RMS deviations in the order of 5 cm (radial) and 15 cm (3D) when excluding the post-manoeuvre period; velocity deviations (see Figure 4) exhibit RMS deviations of 0.3 (along track) and 0.4 mm/s (3D). For the whole period, these numbers are significantly larger due to the convergence of the Metop-B orbit during the first few hours. But even in periods not being disturbed by manoeuvres, they are larger than the nominal requirements which ask for along-track velocity accuracies in the order of 0.1 mm/s.

On the other hand, the deviations found in the operational POD for the Metop-B data are in the same order of magnitude as the deviations between operational and reference orbits in case of Metop-A. The practical experience with GRAS-A data demonstrates that the nominal requirements for POD performance are overly conservative; for GRAS-A, the observed level of orbit accuracy has been demonstrated to be sufficient to produce bending angle data within user requirements.

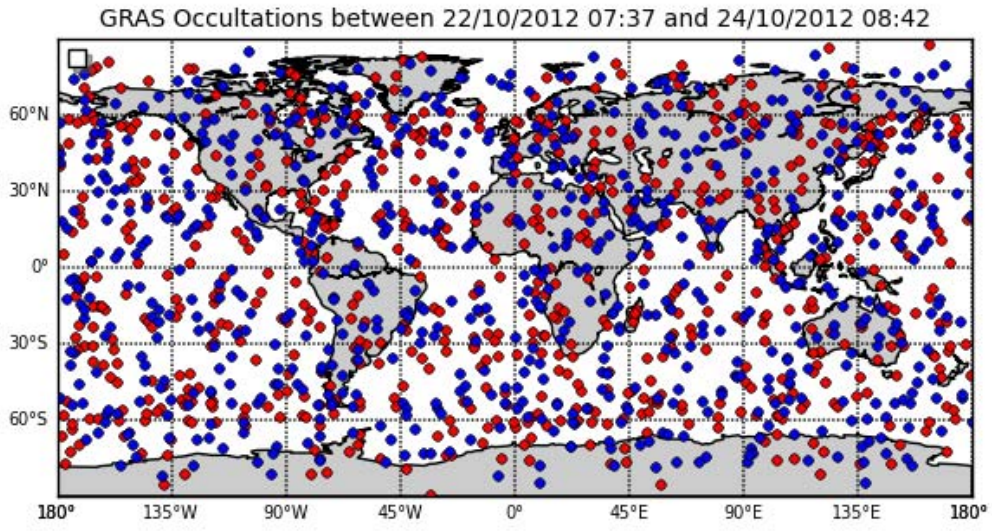

Figure 5: Geolocation of Metop-B GRAS occultations during 48 hours (22nd to 24th October). Setting and rising occultations are denoted by blue and red points, respectively.

These comparison results therefore demonstrate that after a few (expected) hours of convergence, the operational orbit determination component of the GRAS PPF successfully converges to an orbit which has sufficient accuracy for the processing of radio occultation data. Post-manoeuvre periods were indeed the only periods when larger-than-usual deviations between operational and reference POD solutions were observed for Metop-B (as well as Metop-A).

2.1.4 Geolocation

Once the positions of the satellites participating in a radio occultation measurement are known, the geolocation of the occultation measurement is calculated using purely geometrical considerations. Figure 5 shows the locations of rising and setting occultations for 48 hours of Metop-B data as retrieved from the GRAS PPF.

The usual irregular, globally distributed pattern of mixed rising and setting occultations is found, again similar to comparable figures known from Metop-A. The number of occultations is also consistent with the number of occultations obtained from Metop-A during the same period (see also Figure 10).

2.1.5 Upper Level Data Quality Indicators

A prime indicator for assessing radio occultation data quality are upper level bias and noise statistics: If systematic errors exist in the satellite's orbits, velocities or clock bias estimates, they show up in systematic biases of bending angle profiles at high altitudes, with opposite signs for setting and rising occultations. The convergence period of the sequential POD can also often be identified by an increased scatter of upper level bending angle biases.

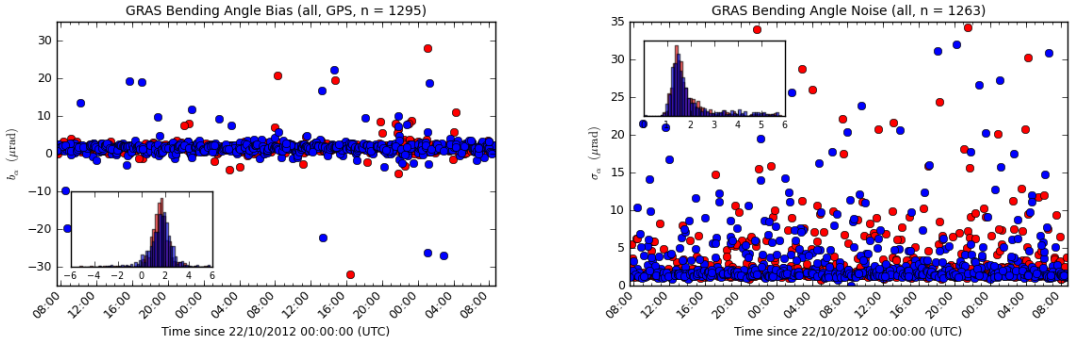

Figure 6: Upper level (60 - 80 km impact altitude) bending angle mean (left) and noise / standard deviation (right) for setting (blue) and rising (red) occultations between 22nd and 24th October. Insets show the frequency distributions of these values over the same period. Note the signature of the manoeuvre in the spread of mean bending angle values after 21:42 UTC on 23rd October in the left figure.

Anomalously increased receiver noise levels (or errors in the ionospheric correction of the bending angle retrievals) show also up as increased noise in the upper level bending angle data.

Figure 6 shows time series and frequency distributions of bending angle mean values and standard deviations over an (impact) altitude range between 60 and 80 km. The expectation for a nominal radio occultation bending angle retrieval would be to exhibit a mean value in the order of 0.5 - 3 µrad, and noise values of typically less than 3-5 µrad. The figure indicates that these expectations are fully met by the GRAS PPF retrievals obtained from the Metop-B data. Also note the increased scatter of mean bending angle values at the manoeuvre time, characteristic for the POD convergence period. We note that the small increase in scatter indicates (as do the direct orbit comparisons shown in Figure 3 and Figure 4) that the POD convergence went exceptionally smooth in this particular case. The histograms demonstrate that the observed upper level bending angle statistics are well within the stated expectations.

Based on previous experience with GRAS-A processing, these findings suggest that the geometrical optics bending angle retrievals calculated from the Metop-B data are likely to be within the accuracy requirements for the GRAS instruments. A more detailed analysis is not possible within the existing operational GRAS PPF, but requires the analysis of results from the GRAS prototype.

2.1.6 Comparison with ECMWF

Bending angle profiles calculated by the operational GRAS PPF from the Metop-B data are compared with bending angles forward modelled from co-located ECMWF short range weather forecast fields as available in the EUMETSAT ground segments. Forward modelling and thinning of retrieved as well as ECMWF bending angle profiles to a common (impact) altitude grid was performed using the ROPP software suite developed by the ROM SAF. Relative deviations are calculated at each impact altitude, using the generally used NWP measure of (O-B)/B, where O is the observation (GRAS), and B is the forward modelled background (ECMWF).

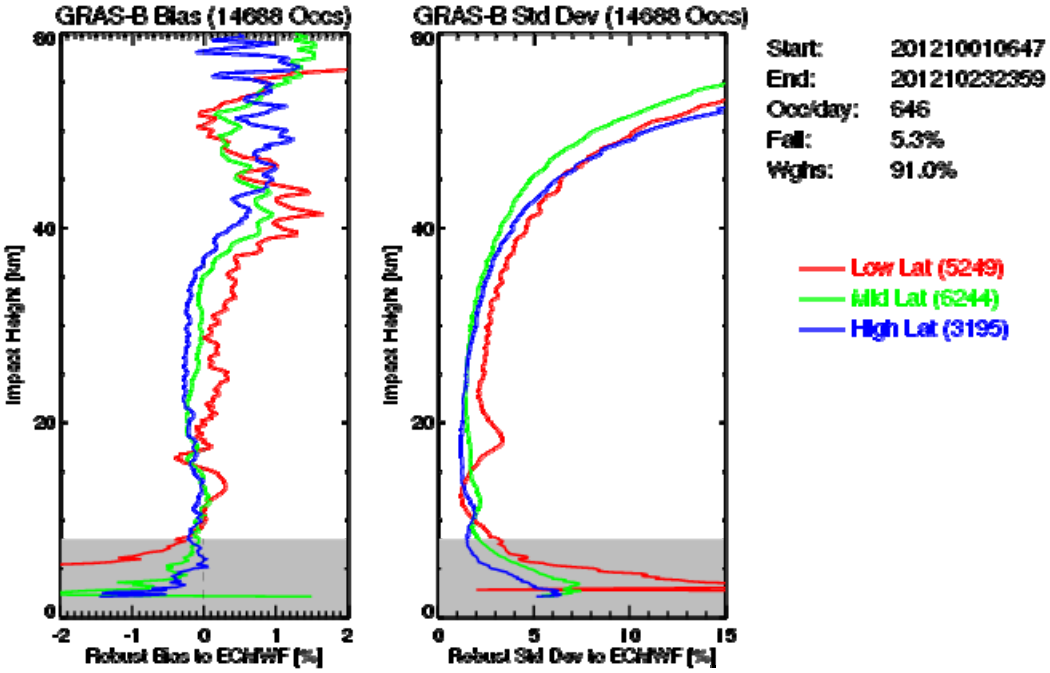

Figure 7: Robust inter-comparison statistics (left: bias, right: spread) against co-located bending angle profiles forward modelled from ECMWF short range weather forecasts for October 2012 Metop-B data. The statistics is stratified into low (red), mid (green) and high (blue) latitude bands, with combined setting and rising occultations. Grey area indicates GRAS geometrical optics processing limitation.

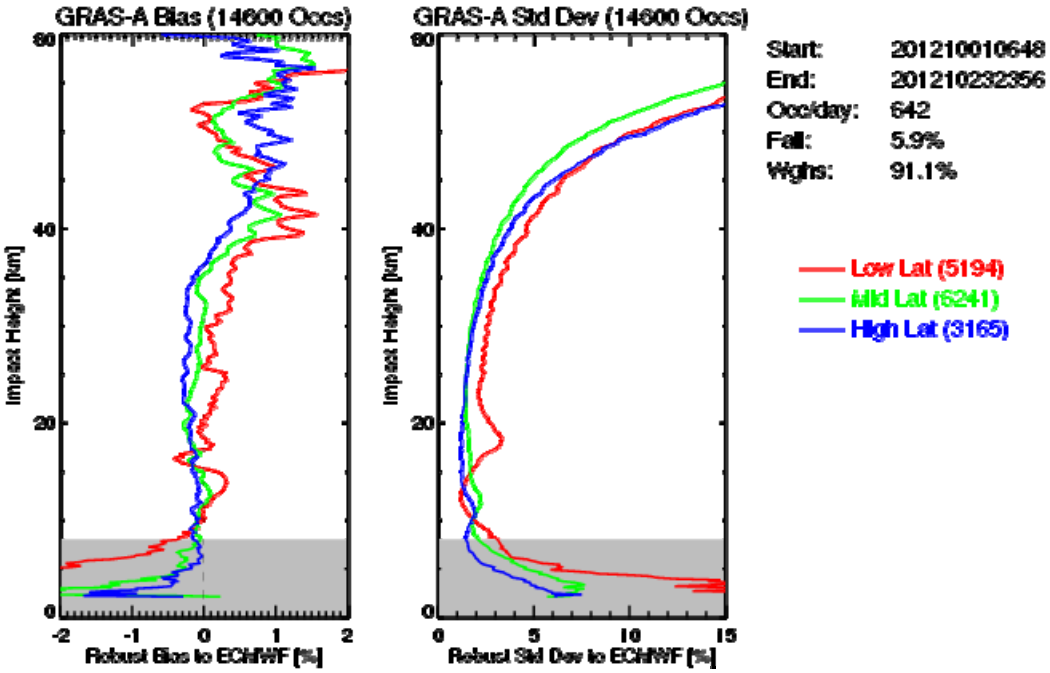

Figure 8: Same as Figure 7 but for Metop-A.

Figure 7 shows robust statistics between retrieved and forward modelled bending angles, stratified by latitude bands. There are almost no apparent biases between 8 and 36 km impact altitude; standard deviations between 15 and 35 km impact altitude are below 2% outside of the tropics. The visible bias is thought to be coming from ECMWF and is not visible in direct GRAS to COSMIC RO data validations (see below). Standard deviations in the tropical lower and mid stratosphere are expectedly higher (up to 3% outside the tropopause region, and even higher close to the tropical tropopause). The latter is caused by radio occultation measurements, due to their better vertical resolution they also include information about the gravity wave spectrum in the tropical stratosphere which is underrepresented in NWP analyses and forecasts. Above about 35 km impact altitude, profiles exhibit slightly larger deviations between GRAS and ECMWF. These are also found in comparisons of ECMWF with COSMIC RO data and are thought to be partly (around 40km) caused by the bias corrections applied to microwave radiance data in the ECMWF data assimilation scheme (S. B. Healy, pers. comm.).

In the lower troposphere, standard deviations increase significantly due to the limitations of the geometrical optics retrieval methodology, which is not suited to represent the complex signal propagation in the moist atmosphere.

Overall, the statistics of bending angle retrievals obtained from the Metop-B data is very similar compared to statistics obtained from Metop-A (as shown in Figure 8 for the same period), confirming that GRAS-B level 1b products are of similar quality as those from GRAS-A.

2.1.7 Comparison with Metop-A

Statistics from the direct comparison between co-located Metop-A and Metop-B bending angle profiles are shown in Figure 9. The calculation follows the same principle as the comparisons against ECMWF, making use of the (O-B)/B statistics, where O is the observation (GRAS-A), and B the background/reference used here (GRAS-B).

The comparison demonstrates that the deviations between co-located Metop-A and Metop-B bending angle profiles at impact altitudes below 40 km are smaller than those found against ECMWF. Above 40 km impact altitude and up to 50 km impact height (which is also the range used for assimilation of the data into e.g., ECMWF), systematic and random deviations are still smaller than ≈1% and ≈15%, respectively.

2.1.8 Comparisons with Metop-A and COSMIC

Figure 10 shows the number of occultations available from Metop-A, Metop-B, and the COSMIC constellation for the investigated period. In addition, the total number of occultations provided by EUMETSAT is shown. COSMIC data was obtained from the UCAR/CDAAC archive of operationally provided occultations. The early dip in Metop-B data availability was caused by the monitoring setup. Otherwise, GRAS on Metop-A and Metop-B provide very similar numbers of occultations, as expected. In total, EUMETSAT provides now similar numbers of occultations as does the full COSMIC constellation (which is beyond its life time and degrading), at least for this period.

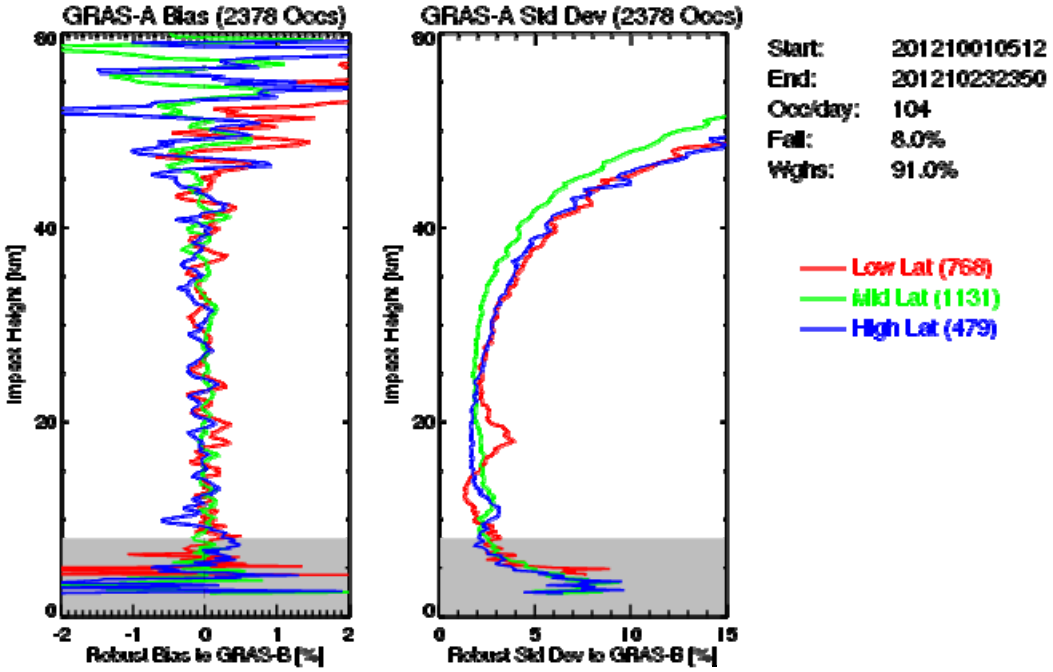

Figure 9: Robust inter-comparison statistics (left: bias, right: spread) against co-located geometrical optics bending angle profiles obtained from GRAS on Metop-A for October 2012 Metop-B data. The statistics is stratified into low (red), mid (green) and high (blue) latitude bands, with combined setting and rising occultations. Co-locations are within ≤ 3h and ≤ 300km. Grey area indicates GRAS geometrical optics processing limitation.

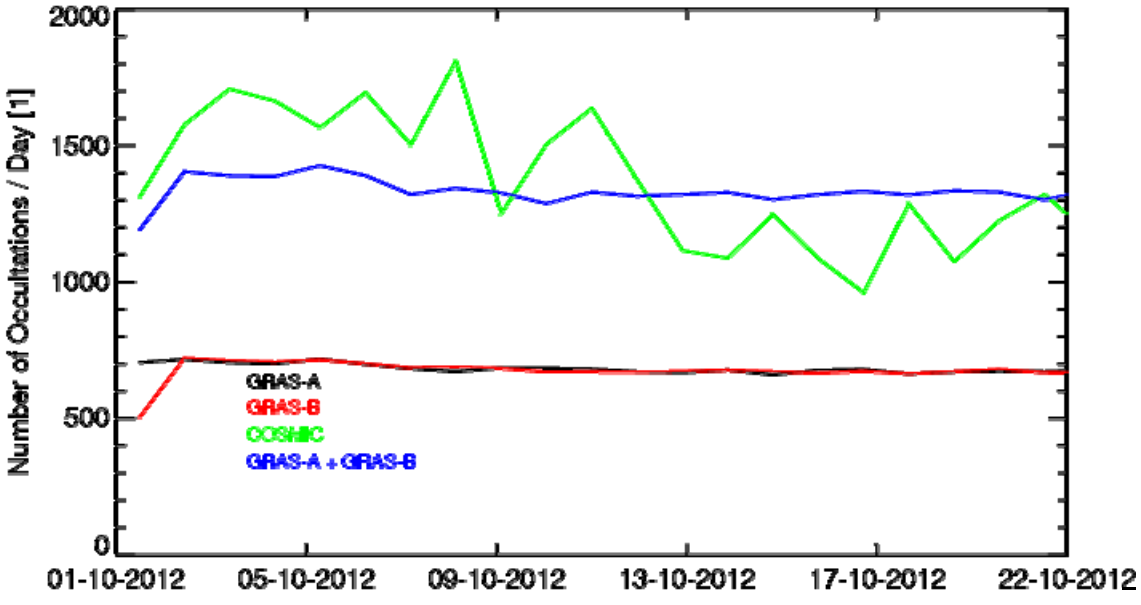

Figure 10: Daily number of occultations available from GRAS on Metop-A, Metop-B, and from COSMIC for October 2012. Total of GRAS occultations is also shown.

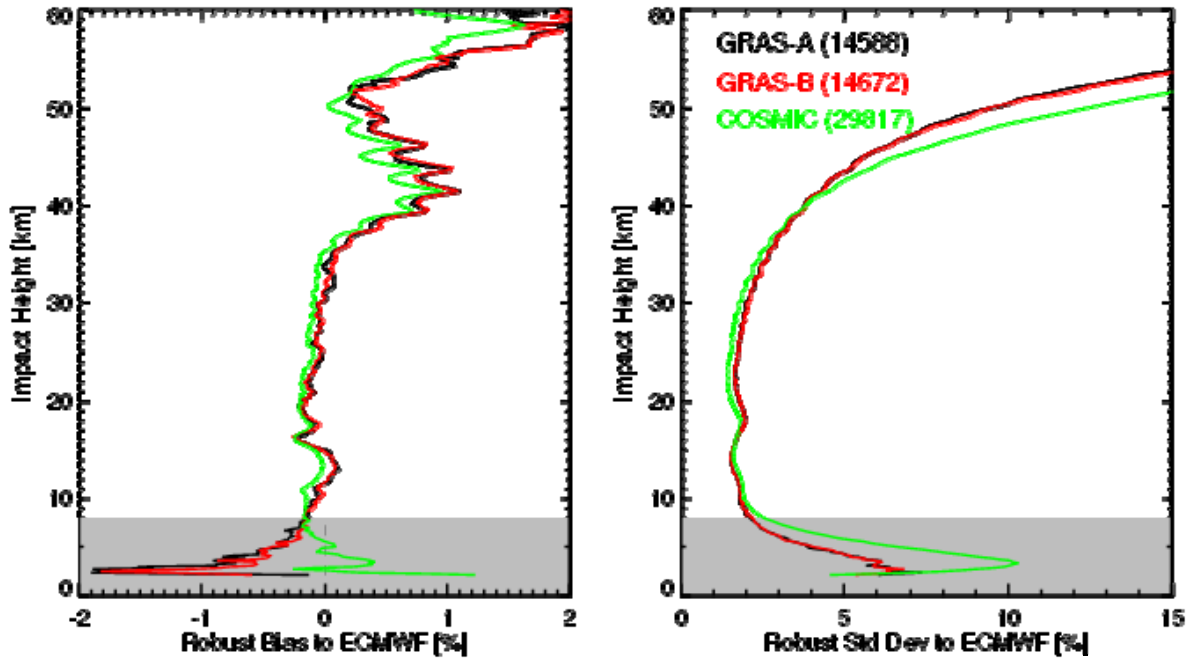

Figure 11: Robust inter-comparison statistics (left: bias, right: spread) against co-located bending angle profiles forward modelled from ECMWF short range weather forecasts for October 2012 data of GRAS-A, GRAS-B, and COSMIC. Grey area indicates GRAS geometrical optics processing limitation. The number of available occultations is shown in brackets.

Figure 11 shows global (O-B)/B statistics of the three observations against ECMWF co-located forecast data. The latitudinal separated GRAS against ECMWF statistics were already shown in Figure 7 and Figure 8. The figure again confirms the high degree of similarity of all three observations against ECMWF, thus several of the visible biases are likely present in the ECMWF model, since they are observed in all investigated radio occultation observations. The slightly higher noise found on the GRAS data between about 15 km to 40 km is thought to be caused by different smoothing applications performed at UCAR/CDAAC and at EUMETSAT. The increased COSMIC noise above about 40 km shows the limitation of single-differencing of COSMIC data. GRAS has an Ultra-Stable-Oscillator, which allows using no differencing (zero-differencing) when processing the data.

Figure 12 shows matches within 300 km and 3 h between the two Metop satellites and the COSMIC constellation, showing the resulting statistics in the same way as the (O-B)/B statistics previously. Note that latitudinal co-locations of Metop-A and Metop-B profiles from the GRAS instruments were already shown in Figure 9, while we present the global statistics in this figure.

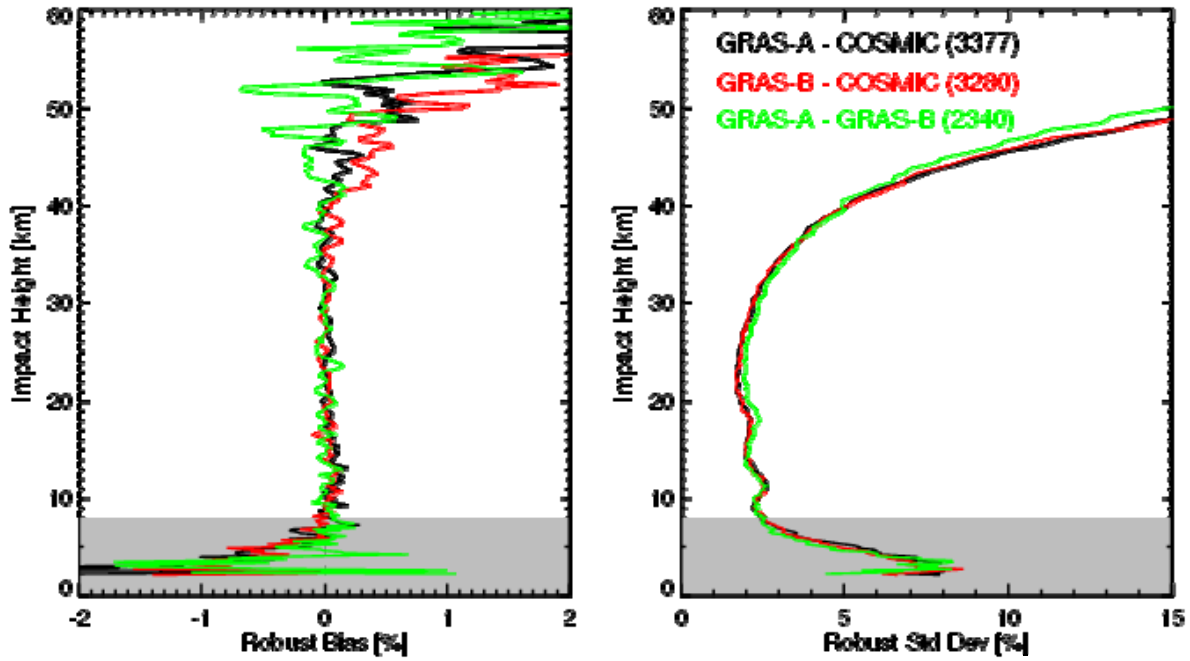

Figure 12: Robust inter-comparison statistics (left: bias, right: spread) against global co-located bending angle profiles for October 2012 data of GRAS-A with COSMIC, GRAS-B with COSMIC, and GRAS-A with GRAS-B. Co-locations are within ≤ 3h and ≤ 300km. Grey area indicates GRAS geometrical optics processing limitation. The number of available occultations is shown in brackets.

The results confirm once more the high degree of agreement between all three observations, with biases between the different instruments for altitudes between 8 km to 40 km smaller than those found against ECMWF (see Figure 11). Above 40 km, a higher degree of bias deviations is observed, this is however still very small compared to the error assignments used in NWP assimilation of this data type. The standard deviation plot shows the expected features, where co-locations with COSMIC exhibit higher noise at altitudes above about 40km, due to single-differencing use in COSMIC data, and lower noise within about 15 km to 35km, due to different smoothing used in COSMIC data.

2.1.9 Timeliness of Occultations

Figure 13 demonstrates that the Metop-B processing is well within the formally required timeliness requirements of 2:15 h.

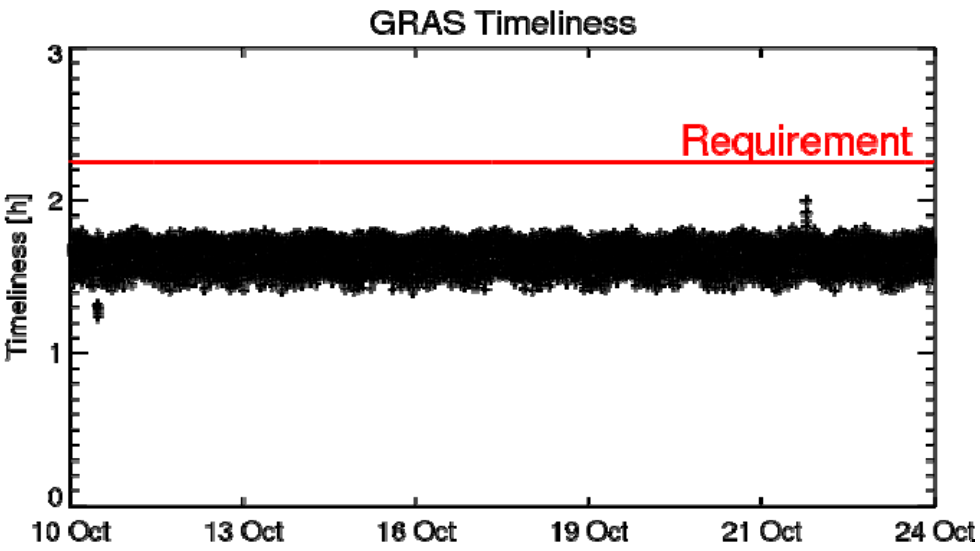

Figure 13: Timeliness of GRAS-B level 1b products from GS1 since 10th October.

2.2 Offline / Prototype Processing

2.2.1 Offline Suite

The GRAS Team currently runs two offline processing chains for every GRAS instrument in Linux virtual server environments. These processing chains generate geometrical optics as well as advanced ("wave optics") bending angle products in future data formats. Data products are also converted into bufr format and are – for GRAS-A – made available to partners in the ROM SAF and the wider global radio occultation community. These activities aim at the early validation of GRAS Day-2 products.

The offline processing is based on revision 2535 of the GRAS / Yaros prototype software that also forms the reference for the upcoming Day-2 GRAS PPF. In contrast to the current operational GRAS PPF, satellite specific instrument characterization databases are fully exploited in the processing, as are raw sampling measurements. The offline processing also contains an advanced ("wave optics") retrieval which is still in development; a number of data quality issues (higher noise levels at high altitudes, and poor performance of the wave optics in low latitudes due to data gaps) are well known and will require further tuning.

2.2.2 Data Availability

The GRAS offline processing is fed through a rolling file buffer for level 0 data from GS1, with data becoming available for the same times as for the operational data processing. Auxiliary data files are also taken from the operational ground segment.

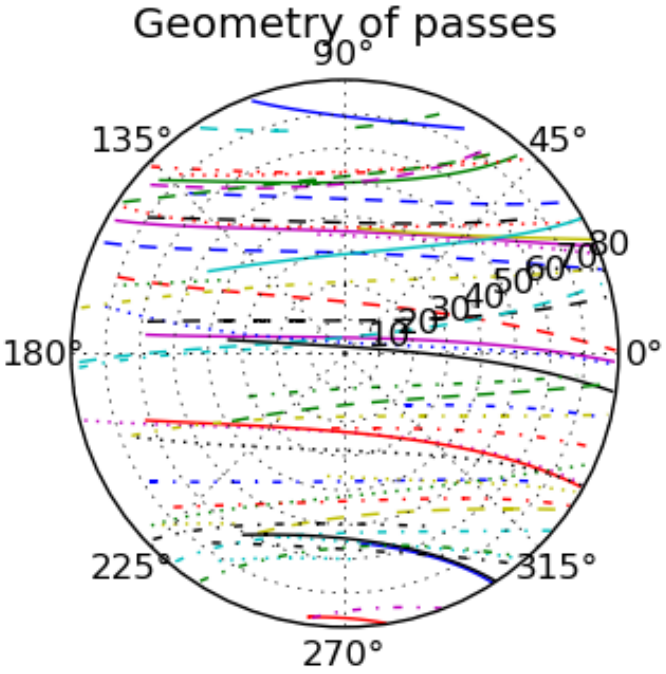

Figure 14: Path geometry of GPS satellites successfully tracked through the GRAS zenith antenna during the first 2 hours of GRAS data on Metop-B, shown as function of azimuth and zenith angle. Note that the satellite is moving towards the left.

2.2.3 Processing

As the operational processing, the offline processing for GRAS-B data worked immediately after the processing had been started. The first level 1b product could be generated by the offline processing chain shortly after the first measurements became available on TCE for both the geometrical optics and the advanced processing chains. An interruption in the processing occurred when data processing was enabled on GS1, and the monitoring and offline processing suites were reconfigured to use GS1 auxiliary and product data. Otherwise, GRAS-B data has been processed continuously without further interruptions. All level 1b products produced by the offline processing were successfully converted into WMO bufr.

2.2.4 Zenith Data and POD Performance

Figure 14 shows the GPS satellites being tracked by the GRAS POD antenna during the first two hours of Metop-B operations as function of azimuth and elevation. The figure was obtained from the diagnostic output of the POD component used in the GRAS offline processing, and demonstrates that GRAS tracks GPS satellites down to 10° elevation as specified by the instrument requirements). We note that the offline POD is a batch POD with the same configuration as used in the monitoring of the GRAS PPF orbit solution described earlier. It can be regarded as a reference solution when compared with EUMETSAT's operational processing chain. In order to simulate NRT timeliness requirements in the offline processing as much as possible, the process is simply run more often than in the monitoring suite.

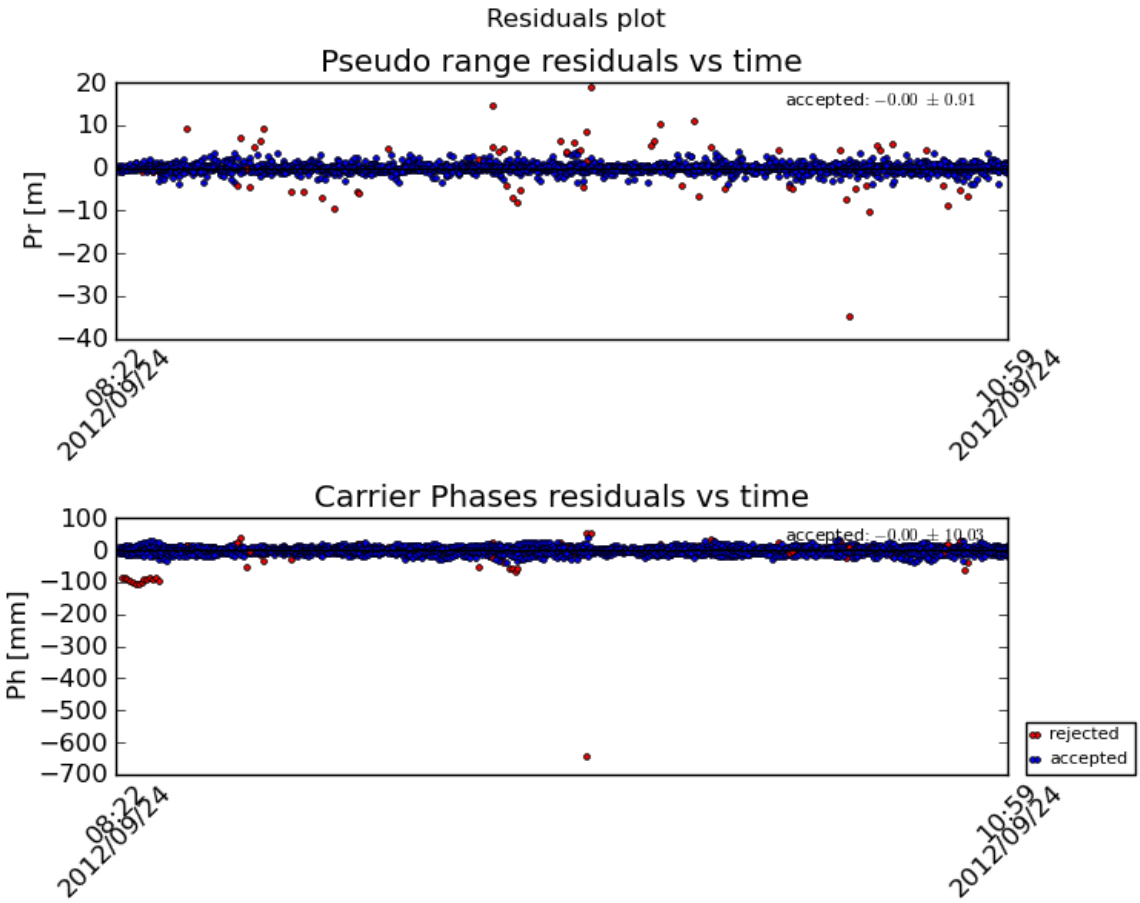

Figure 15: Time series of pseudo-range (top) and carrier phase (bottom) residuals during the first 2 hour POD run. Data points not being accepted by the POD's quality control are shown in red.

Time series of the pseudo-range and carrier phase residuals from the same POD run (covering the first two hours of GRAS-B data) are presented in Figure 15. The results show unbiased pseudo-range and carrier phase measurements from Metop-B with random errors in the order of 90 cm and 1 cm, respectively, in very good agreement with Metop-A data. This suggests once more that POD solutions should be of similar accuracy as those obtained from GRAS on Metop-A.

Neither the tracking behaviour of the GRAS-B instrument nor the error characteristics of its measurements have changed since then. The continuing excellent tracking performance of the GRAS-B instrument can also be demonstrated by showing the number of tracked GPS satellites as in Figure 16. Since the first GRAS-B data became available, the receiver continuous to nearly always track 7 or 8 GPS satellites at the same time, thus always providing sufficient amount of zenith antenna data for performing a POD.

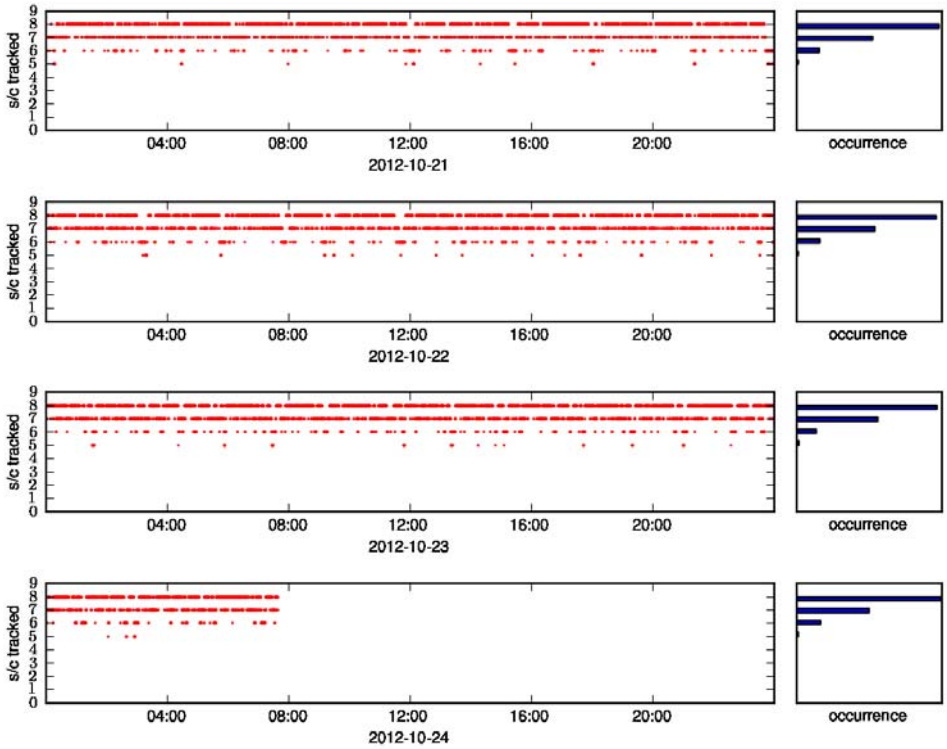

Figure 16: Number of GPS satellites being simultaneously tracked by the GRAS-B zenith antenna from 21st to 24th October. Bar charts on the right show relative frequencies.

2.2.5 Occultation Data Performance

Figure 17 shows histograms of the C/A and L2/P upper level global SNRs for the GRAS instruments on both Metop-A and Metop-B between 25th September and 24th October 2012. The analysis confirms that GRAS on Metop-B provides slightly smaller SNR values compared to GRAS-A on average; for C/A carrier phases, Metop-A and –B exhibit median SNRs of 821 V/V and 787 V/V, respectively (271 V/V and 255 V/V, respectively, for L2/P). In C/N_0, this corresponds to difference of 0.4 dB for both frequencies.

An independent estimate of carrier phase noise (Figure 18) confirms marginal differences between Metop-A and -B, with C/A noise values of 0.296 mm and 0.302 mm, respectively (0.888 mm and 0.931 mm for L2/P). These differences, in our experience, will not cause measurable differences in bending angle performance, consistent with the validation results shown above.

Meridional SNR distributions (Figure 19) for the GRAS instruments on both Metop-A and Metop-B show the known sensitivity of the instrument's noise estimation algorithms to radar induced RF background noise in the Northern Hemisphere. Apart from the overall slightly lower SNR level in Metop-B data, the shape of the distribution is rather similar, once more confirming that the two GRAS instruments exhibit very similar measurement characteristics.

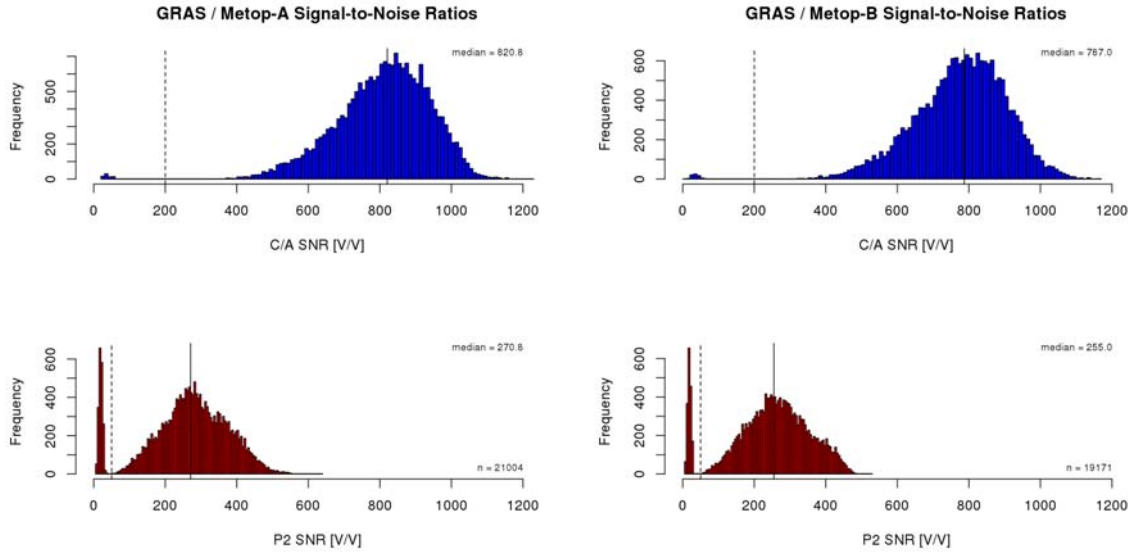

Figure 17: Frequency distributions of C/A (top) and L2/P (bottom) carrier phase SNRs for GRAS on Metop-A (left) and Metop-B (right) for one month (25th September – 24th October 2012) of Metop-B data. Straight vertical lines indicate the median SNR values (see text); dashed vertical lines indicate quality control thresholds as applied in the GRAS processing prototype.

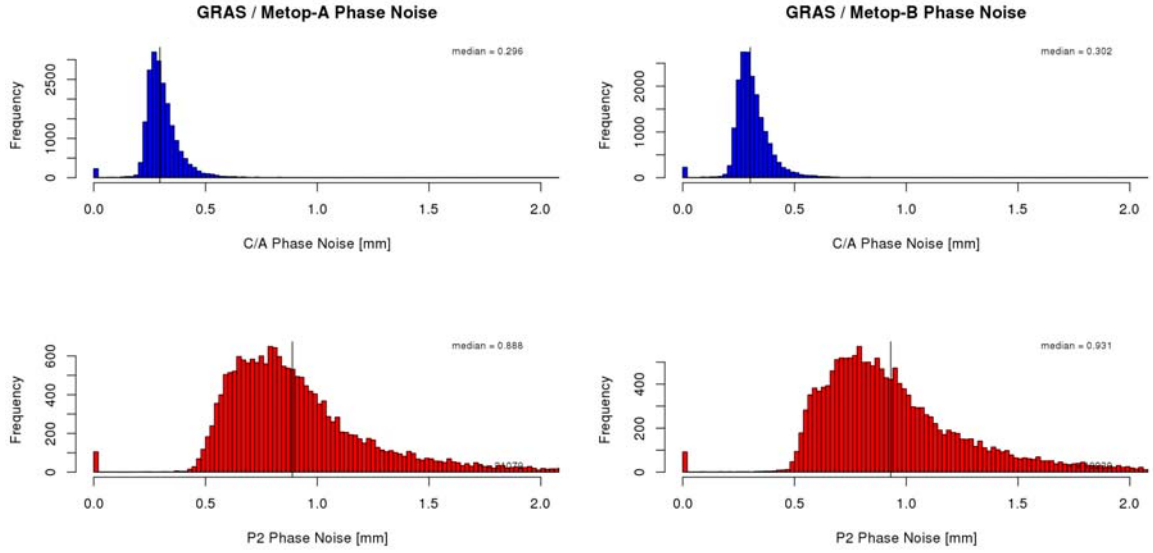

Figure 18: Frequency distributions of C/A (top) and L2/P (bottom) carrier phase noise as estimated with Generalized Cross Validation Spline Fits for GRAS on Metop-A (left) and Metop-B (right) for one month (25th September – 24th October 2012) of Metop-B data. Straight vertical lines indicate the median phase noise values.

With respect to penetration into the troposphere, meridional pattern are also similar between the instruments. Figure 20 shows the SLTA frequency distribution of the lowest observed open loop data as for both rising and setting occultations. It is known from the analysis of deep occultation with GRAS on Metop-A that the upper banana shaped region reflects the

onset of atmospheric information in the GRAS data, while the maxima at and slightly above -250 km SLTA mostly reflect cross PRN tracking events in rising occultations. The figure also confirms that both instruments are operated with identical lower SLTA settings with a measurement cutoff of -250 km SLTA.

An analysis of the known deficiencies of the GRAS receiver was also undertaken based on the first month of Metop-B data (25th September to 24th October). Initial results from the first version of this report were confirmed; in particular, GRAS on Metop-B suffers from

- a significant number of cases exhibiting closed loop data gaps in rising occultations (37.7% of rising occultations on Metop-B, compared to 37.1% on Metop-A);
- a small number (9.1%) of occultations with poor L2/P tracking (9.2% for Metop-A);
- regular data gaps in open loop observations (nearly all occultations, as for Metop-A).

We note that both the number of closed loop data gaps and cases with poor L2 tracking are slightly higher than expected from previous studies which mostly concentrated on a one month period in 2007. The small inter-satellite differences in the statistics are considered to be due to different sampling.

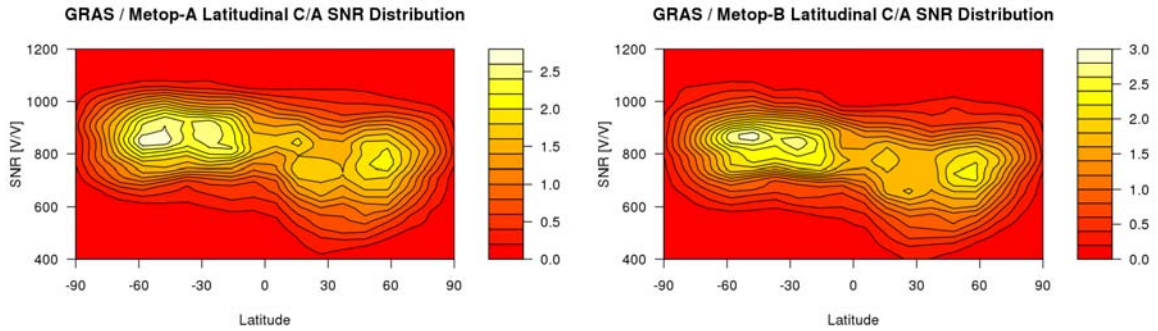

Figure 19: Meridional frequency distribution of C/A carrier phase SNRs between 24th September and 24th October 2012 GRAS on Metop-A (left) and Metop-B (right). Frequency units are arbitrary.

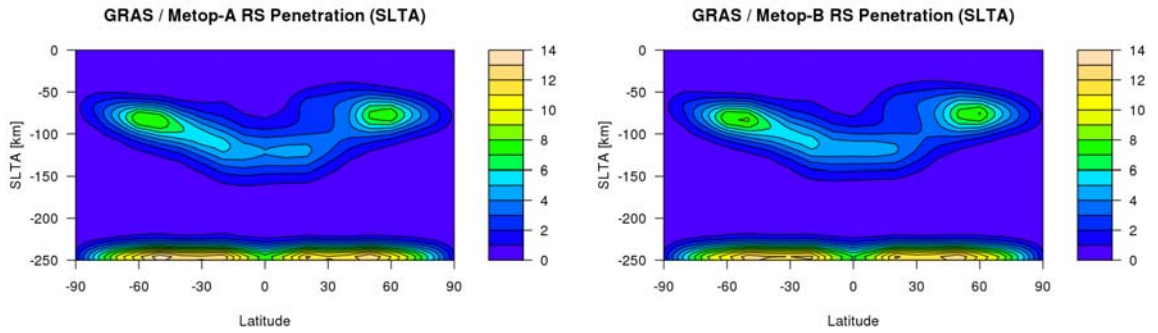

Figure 20: Altitude of the lowest open loop observation as function of SLTA between 25th September and 24th October 2012 for GRAS on Metop-A (left) and Metop-B (right). Frequency units are arbitrary.

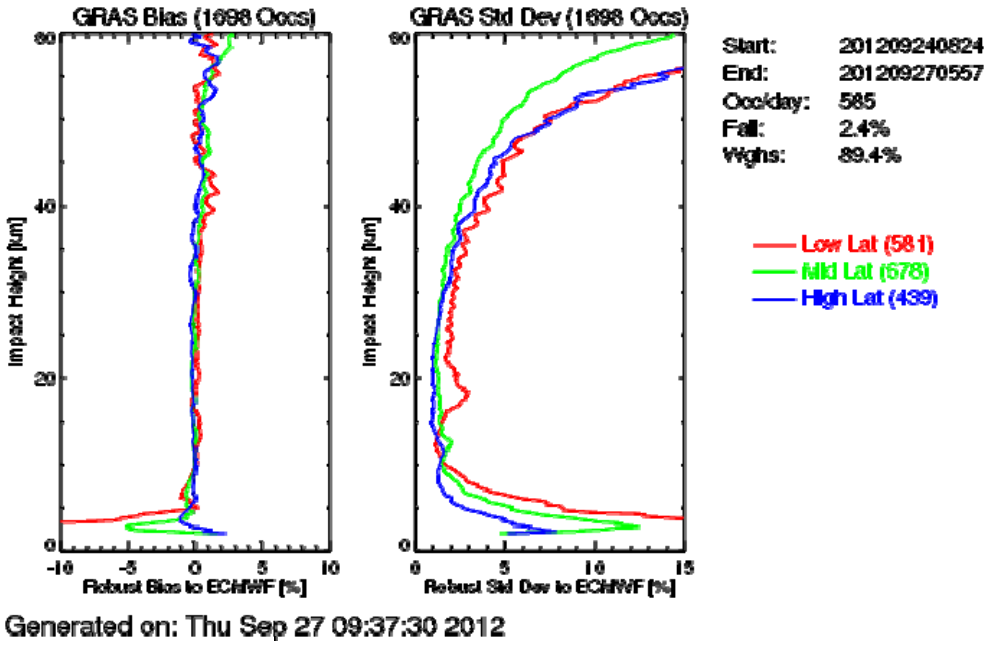

Figure 21: Robust inter-comparison statistics (left: bias, right: spread) of geometrical optics offline products against co-located bending angle profiles forward modelled from ECMWF short range weather forecasts for the first 72 hours of Metop-B data. The statistics is stratified into low (red), mid (green) and high (blue) latitude bands, with combined setting and rising occultations.

2.2.6 Comparison with ECMWF

Similar to the monitoring of the operational processing, latitudinally stratified statistical inter-comparisons between GRAS-B offline products and forward modelled ECMWF bending angles were performed, and are presented in Figure 21.

The figure shows statistics from the geometrical optics processing chain, where the agreement between offline products and ECMWF data is even better than for the operational products at high altitudes. This confirms earlier, similar results obtained during the prototype development. Latitudinal differences in the lower and mid stratosphere are similar to those observed in the operational processing. In contrast to the operational PPF, the offline processing also extrapolates L2 measurements further downwards, emphasizing the limitations of the geometrical optics retrieval approach in the troposphere.

The implementation of advanced retrieval methods is still under development, and therefore not further discussed in this report.

3 EXTERNAL PARTNER VALIDATION

3.1 Scope of Validation

External validation activities focussed on two areas:

- Quality of the operational and reference POD solutions for Metop-B
- Quality of the operational GRAS / Metop-B level 1 data products

A. Hauschild (DLR/GSOC) was a available as visiting scientist between 26th September and 4th October, concentrating on the POD issues; with the start of the trial dissemination of 28th September ECMWF, Met Office (both part of the ROM SAF), DWD and Météo France studied data quality of GRAS level 1 products from Metop-B, and have partially integrated the data flow in their respective monitoring systems.

3.2 Validation Results - DLR

Andre Hauschild (DLR) provided a written report [RD-2] describing his results in detail; apart from more comparisons with EUMETSAT's reference orbit, he also provided results on the Signal-to-Noise Power Density ratio, an in-space zenith antenna phase centre calibration as well as a characterisation of the GRAS / Metop-B clock.

The main results of his work are

- the reference orbit solution produced at EUMETSAT agrees with the DLR solution within a few cm, i.e. compares at the same state-of-the-art level as for Metop-A;
- carrier phase and pseudo range residuals are in the same order as those diagnosed by the EUMETSAT reference POD system;
- phase centre variations are similar, but not equal to Metop-A, and their application in POD reduces the observed carrier phase residuals significantly (as they do for Metop-A);
- the temperature dependency of the GRAS-B clock during the initial two weeks of Metop-B data was larger than for Metop-A at the same time, although still within the stated requirements. The observed temperature dependency did however weaken during the analysis period and converged towards the long-term values observed for GRAS-A, suggesting that the initial behaviour improves with the aging of the clock oscillator;
- Allen deviation of the GRAS-B clock is slightly worse than for Metop-A (and actually slightly out of specification), but also improved over a sequence of a few days, again suggesting that the quartz oscillator needs a period of aging before it fully performs within requirements.

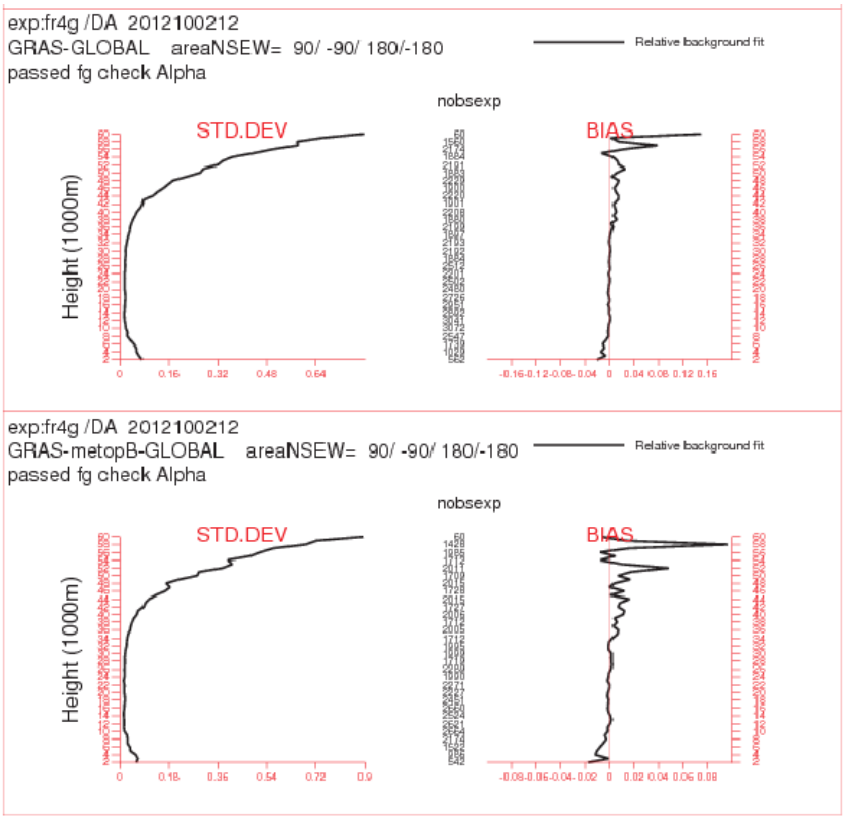

Figure 22: Bending angle standard deviations (left) and bias (right) of quality controlled GRAS data against ECMWF short range forecasts for Metop-A (top) and Metop-B (bottom) for 10 days (figures courtesy Sean Healy, ECMWF).

The GRAS team will continue to monitor the clock behaviour as soon as the required analysis tools have been implemented. Due to the quality of the POD and clock solutions in both offline and operational processing, however, the slightly poorer behaviour of the GRAS-B clock is not considered to have a significant impact on GRAS level 1 product quality.

3.3 Validation Results – ECMWF

Sean Healy provided both ordinary validation statistics of GRAS-B against ECMWF short range forecasts for a ten day period (1st – 10th October; Figure 22) as well as normalised (by assumed observation error) statistics against short range forecasts and analyses (for the same period; Figure 23), confirming the validation results obtained internally at EUMETSAT. The agreement of Metop-A bending angle profiles with ECMWF analyses is better than with short range forecasts as the data set is already assimilated in the operation ECMWF system; no such improvement is seen for Metop-B data which is only passively monitored. According to Sean, this suggests that improvements in the NWP analysis can be expected from assimilating GRAS data on Metop-B, and first data assimilation experiments with Metop-B data have indeed been started at ECMWF. The passive monitoring of GRAS-B data is also available on ECMWF's monitoring web pages.

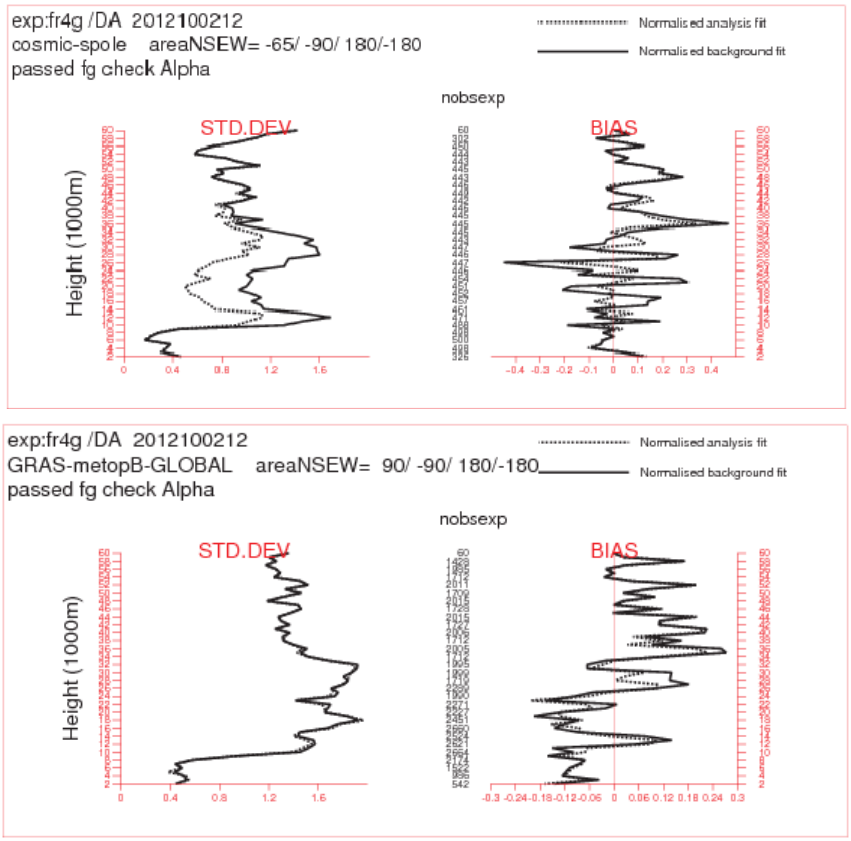

Figure 23: Normalised bending angle standard deviation (left) and bias (right) of quality controlled GRAS data against ECMWF short range forecasts and analyses for Metop-A (top) and Metop-B (bottom) for 10 days (figures courtesy Sean Healy, ECMWF).

3.4 Validation Results – Met Office

Initial validation results provided by Chris Burrows (Met Office) are shown in Figure 24. The statistics once more confirm internal validation results for the quality controlled data. The bias structure above 35 km altitude deviates from the comparisons against other NWP data (e.g. ECMWF) due to different model biases at stratospheric model levels. According to Chris, preparations for initial data assimilation experiments are underway to be carried out in the shadow suite of the Met Office; the monitoring statistics will also be added to the ROM SAF's monitoring pages in the near future.

3.5 Validation Results – DWD

Harald Anlauf provided comparison statistics for both Metop-A and Metop-B data for the first 12 days of Metop-B data (29th September to 10th October; Figure 25), demonstrating that data from the two GRAS instruments are virtually indistinguishable by their statistics against DWD short range forecasts. Data assimilation trials for Metop-B data are also under discussion at DWD.

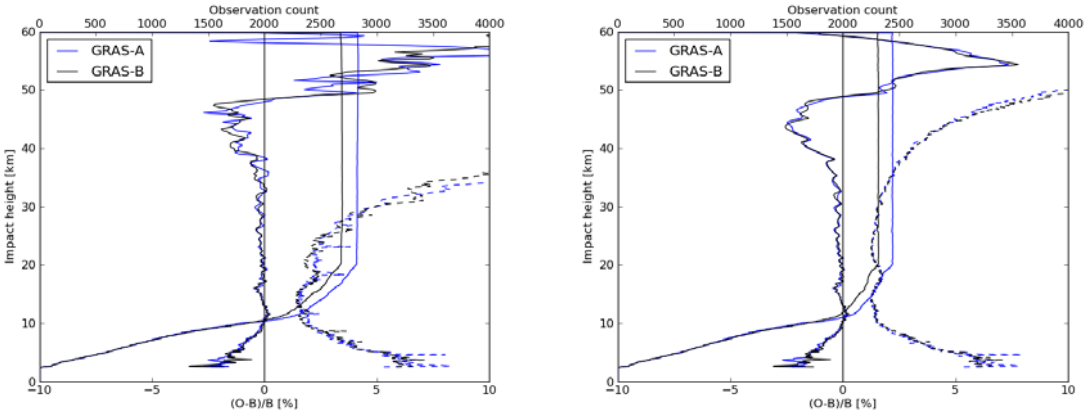

Figure 24: Bending angle standard deviation (dashed) and bias (solid) against Met Office short range forecasts from GRAS on Metop-A (blue) and Metop-B (black) for all (left) and all quality-controlled (right) data (figures courtesy Chris Burrows, Met Office).

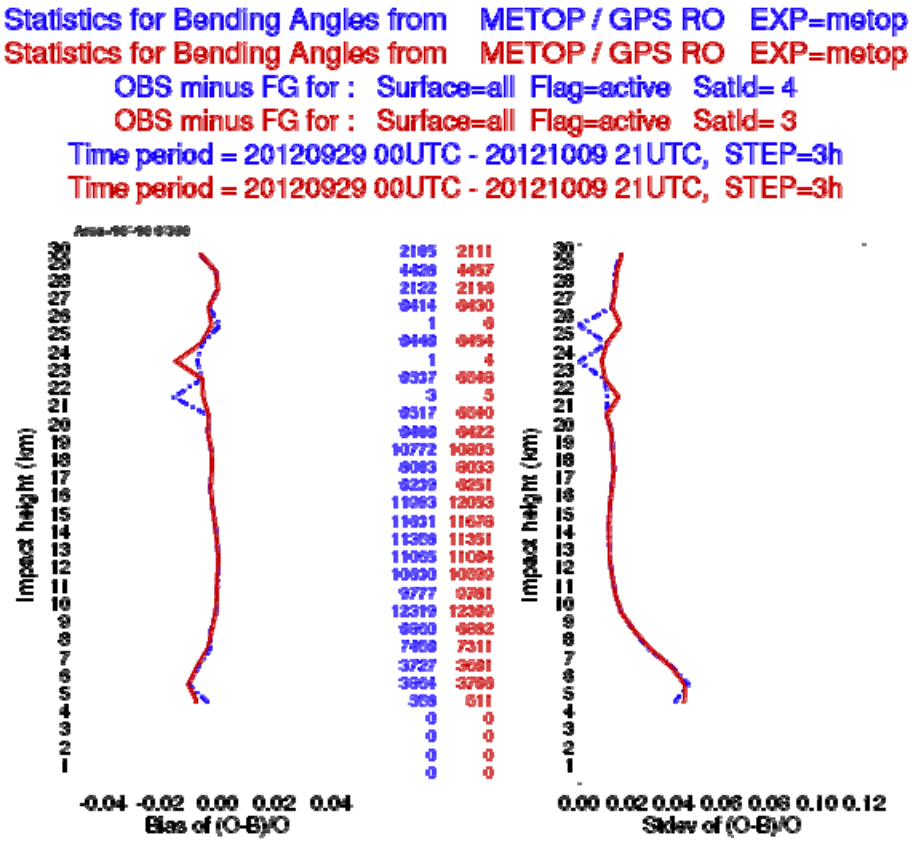

Figure 25: Bending angle bias and (left) and standard deviations (right) of quality controlled GRAS data against DWD short range forecasts for Metop-A (blue) and Metop-B (red; figure courtesy Harald Anlauf, DWD).

3.6 Validation Results – Météo France

Nathalie Saint-Ramond (Météo France) provided a written validation report [RD-3] covering a 15 day period (3rd – 18th October), concluding:

> "For the time period considered here, the quality of GRAS data from Metop-B seems to be close to the quality of Metop-A when compared to our global model. The next step for us will be to make some assimilation experiments. We are looking forward to receiving level 2a product from the ROM SAF with refractivity values, as we need this product to make some screening tests before assimilation."

An interesting detail of the Météo France results is that Metop-B bending angles, compared to Metop-A bending angles, perform slightly worse against Météo France short range forecasts in the altitude range between 25 and 45 km. This somewhat contradicts the findings of the other validation activities. The report notes that Metop-A bending angles were taken from ROM SAF products; a possible explanation for the inconsistent results at Météo France could be small discrepancies of the bending angle products provided by EUMETSAT and the ROM SAF. An intercomparison between ROM SAF and EUMETSAT bending angle products should therefore be undertaken as part of the ROM SAF validation activities for their Metop-B products.

4 CONCLUSIONS

4.1 Product Validation Summary

The assessment of the quality for GRAS-B POD data for both operational and offline processing is within the accuracy required for successful radio occultation processing. Deviations are on the same order as regularly observed for the operational processing of GRAS-A data, suggesting that higher level products will be of similar quality as GRAS-A data.

Comparisons of GRAS level 1b products (bending angle profiles) from Metop-B with ECMWF short range forecasts do indeed demonstrate that GRAS-B products are comparable in quality with GRAS-A data; the statistics with ECMWF short range forecasts cannot be distinguished between the two instruments. We therefore conclude that GRAS-B data is of nominal (operational) quality.

These results are confirmed by comparisons with an external Metop-B orbit estimate independently provided by DLR, as well as bending angle (level 1b) validation activities carried out by ECMWF, Met Office, DWD, and Météo France. All NWP centres participating in the validation activities also informed us that data assimilation trials using GRAS-B data are either planned, or have already started. Regular monitoring statistics is available from both ECMWF and the Met Office.

Independent processing and validation with products generated from the GRAS offline / prototype processing chain also confirm these conclusions. They also suggest that GRAS on Metop-B suffers from the same issues as the instrument on Metop-A, in particular data gaps in closed loop (38% of all rising occultations) and raw sampling data (nearly all occultations)

as well as a significant part of the available occultations with L2/P tracking failures (11 % of all occultations). These issues were expected; a parameter testing campaign tentatively scheduled for the first half of December 2012 will address these issues.

An unexpected result of the early Cal/Val activities for GRAS-B is that the percentage of profiles being affected by these issues is slightly higher than expected for both instruments. A longer period of data should be processed and analysed in order to understand if these numbers reflect a true trend in the instrument behaviour, or are an artefact of the periods being analysed.

Another unexpected result from these activities is that GRAS-B carrier phase measurements on the occultation chains exhibit slightly lower SNR values than GRAS on Metop-A. Carrier phase noise, however, only seems to be affected marginally. There is also no apparent impact on level 1b data quality. This finding therefore has no impact on the recommendation to declare the GRAS level 1 product status as "pre-operational".

In terms of value for users, the availability of GRAS-B data will mainly mean that about twice as much high quality radio occultation data will be available from the "GRAS constellation"; the difference in daily coverage is shown in Figure 26.

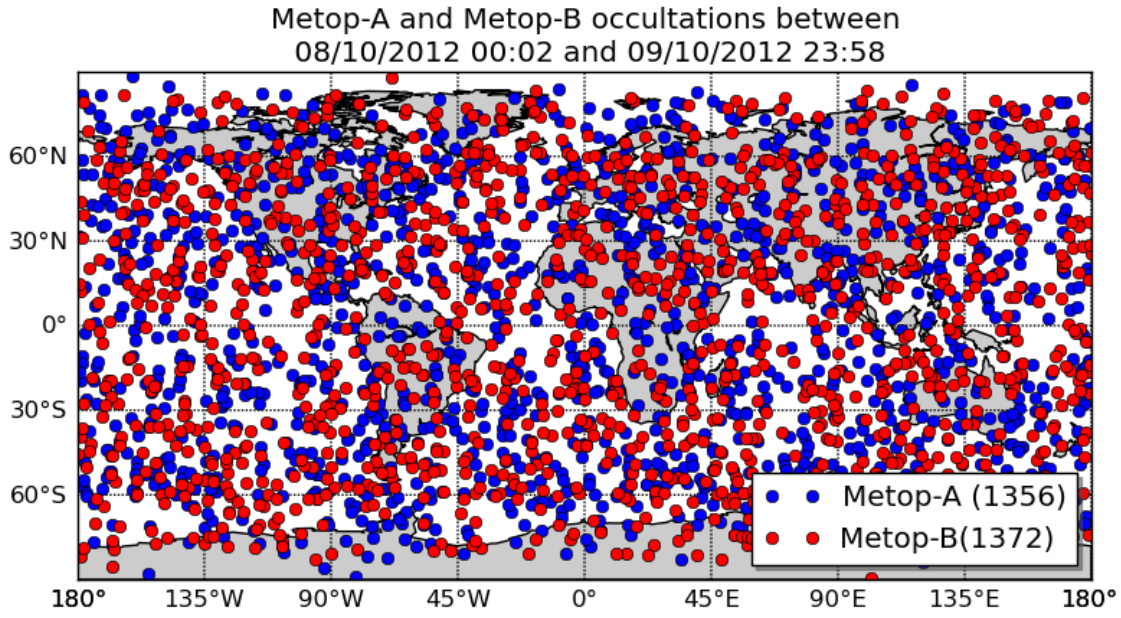

Figure 26: Distribution of radio occultation data from both GRAS instruments during two days in October 2012. Blue and red points indicate Metop-A and Metop-B data, respectively.

4.2 Product Validation Issues

As expected, GRAS on Metop-B suffers from the same issues as GRAS on Metop-A; for details, see Section 2.2.5:

- a significant number of cases exhibiting closed loop data gaps in rising occultations (37.7% of rising occultations on Metop-B, compared to 37.1% on Metop-A);
- a small number (9.1%) of occultations with poor L2/P tracking (9.2% for Metop-A);
- regular data gaps in open loop observations (nearly all occultations, as for Metop-A).

A parameter testing campaign tentatively scheduled for the second half of January 2013 will address these issues.

4.3 Perspectives and Future Work

The scientific validation of GRAS products will continue in the following months, in particular after the parameter test campaign which aims at reducing the number of data gaps and false L2 tracking events. An updated version of this product validation report will be made available if an improved onboard parameter set has been identified and thoroughly validated. This will include a long-term monitoring of the SNR levels for both instruments.

The ROM SAF will address possible inconsistencies in GRAS bending angle data between EUMETSAT and ROM SAF products as part of the validation activities for their GRAS-B products.

In addition, member state NWP agencies will undertake data assimilation studies exploiting the GRAS-B data in their operational systems.

5 RECOMMENDATION

We recommend to the PVRB to change the status of GRAS-B level 1b products to “pre-operational” and to approve the start of the global dissemination of GRAS level 1b products.

6 ACKNOWLEDGMENTS

We are very grateful to A. Hausschild (DLR), S.B. Healy (ECMWF), C. Burrows (MetO), H. Anlauf (DWD), and N. Saint-Ramond (Météo France) for their cooperation on the validation of early Metop-B GRAS data, their quick provision of initial results, and their useful contributions to this report.